Vascular Cell Glycocalyx-Mediated Vascular Remodeling Induced by Hemodynamic Environmental Alteration

Jiajia Liu, Hongyan Kang, Xuejiao Ma, Anqiang Sun, Huiqin Luan, Xiaoyan Deng, Yubo Fan

Abstract—Vascular remodeling induced by hemodynamic stimuli contributes to the pathophysiology of cardiovascular diseases. The importance of vascular cells (endothelial cells and smooth muscle cells) glycocalyx in the mechanotransduction of flow-induced shear stress at the cellular and molecular levels has been demonstrated over the past decade. However, its potential mechanotransduction role in vascular remodeling has triggered little attention. In the present study, a home-made apparatus was used to expose the rat abdominal aorta to sterile, flow or no flow, normal-pressure or high-pressure conditions for 4 days. The histomophometric, cellular, and molecular analysis of vessels were performed. The results showed that after exposing the vessels in the flow and high-pressure condition, the apoptotic rate, the cell number, and the RNA level of contractile marker gene smooth muscle 22 of smooth muscle cells were significantly increased, whereas the expression of nitric oxide synthase, α-smooth muscle actin, smoothelin, and calponion showed no significant differences compared with the flow and normal-pressure groups. Moreover, the histomophometric analysis of vascular walls suggested a remodeling induced by flow and high-pressure loading consistent with the classic hypertensive aortic phenotype, which is characterized by a thicker and more rigid vascular wall as well as increased aortic diameter. However, those phenomena were totally abolished after compromising the integrity of glycocalyx by the treatment of vessels with hyaluronidase, which provided evidence of the important mechanotransduction role of the vascular cells glycocalyx in vascular remodeling induced by hemodynamic stimuli. **(*Hypertension*. 2018;71:00-00. DOI: 10.1161/HYPERTENSIONAHA.117.10678.)** ● **Online Data Supplement**

Key Words: hypertension ■ glycocalyx ■ mechanotransduction, cellular ■ myocytes, smooth muscle ■ vascular remodeling

Vascular remodeling is a complex process that occurs in response to long-term changes in the dynamic interaction between locally generated growth factors, vasoactive substances, and hemodynamic stimuli.[1] For earlier years, the term vascular remodeling was only used to describe a modification of vascular lumen diameter and cross sections associated with rearrangement of material (eg, the apoptosis, migration and proliferation of SMCs [smooth muscle cells], and production or degradation of extracellular matrix).[2,3] However, with recent research, it also represents the process of functional alteration that involves in the change of vasodilative and vasoconstrictive ability,[4,5] the degradation of endothelial function,[6] and the derangements of NOS (nitric oxide synthase) pathway.[7] As an adaptive process in response to the changes in hemodynamic conditions, vascular remodeling is critical during both physiological such as ovarian and uterine cycling,[8] wound healing,[9] endurance-type exercise[10] conditions, and pathophysiology[11] such as atherosclerosis, hypertension, pheochromocytoma, acromegaly, and primary aldosteronism.

Many biomechanical and biochemical factors are associated with the presence of vascular remodeling, including hemodynamic disturbances, exceedingly expression of inflammatory modulators,[12] levels of oxidative stress,[13] autonomic nerve dysfunction,[14] and vasoactive substances regulated by the renin–angiotensin system. Among these factors, the key roles of hemodynamic disturbances in vascular remodeling have been demonstrated by experimental and clinical events. For example, an in vivo work performed by Korshunov and Berk[15] showed that after ligating the left external and internal carotid branches for 1 week, the left and right carotid artery morphological remodeling in response to blood flow changes was observed. Moreover, they performed correlation analysis, indicating that the remodeling was more likely because of primary changes of shear stress in the vessel wall.[15] Although the morphological changes in multiple kinds of arteries during vascular remodeling have been well documented, the underlying molecular mechanisms are still unclear.

The glycocalyx of the endothelial cells (ECs) and SMCs is a surface layer composed primarily of proteoglycans with their associated glycosaminoglycan that includes heparan sulfate, chondroitin sulfate, and hyaluronic acid (HA) and

Received November 29, 2017; first decision December 16, 2017; revision accepted March 23, 2018.

From the Key Laboratory for Biomechanics and Mechanobiology of Ministry of Education, School of Biological Science and Medical Engineering, Beihang University, Beijing, China (J.L., H.K., X.M., A.S., X.D., Y.F.); National Research Center for Rehabilitation Technical Aids, Beijing, China (H.L., Y.F.); and Beijing Advanced Innovation Center for Biomedical Engineering, Beihang University, China (J.L., H.K., X.M., A.S., X.D., Y.F.).

The online-only Data Supplement is available with this article at http://hyper.ahajournals.org/lookup/suppl/doi:10.1161/HYPERTENSIONAHA.117.10678/-/DC1.

Correspondence to Hongyan Kang, School of Biological Science and Medical Engineering, Beihang University, Beijing, China. E-mail hongyankang@buaa.edu.cn or Yubo Fan, National Research Center for Rehabilitation Technical Aids, Beijing, China. E-mail yubofan@buaa.edu.cn

glycoproteins bearing acidic oligosaccharides with terminal sialic acids.[16] Because the evidence that glycocalyx could sense the mechanical forces of blood flow was provided,[17] numerous studies have been performed to identify the importance of glycocalyx mechanotransduction in cardiovascular physiology and pathology in the past 2 decades. It has been demonstrated that the glycocalyx might participate in modulating cell proliferation, migration, and NO production by sensing shear stress[18] and play a dominant role in 3-dimensional (3D) interstitial flow mechanosensing to modulate SMC phenotype gene expression[5] and motility.[19] In addition, our previous study has suggested that the redistribution of hemodynamic factors in tail-suspended rats could induce their vascular endothelial glycocalyx and the vascular remodeling in a regional-dependent manner, which provided the evidence of some possible association between the endothelial glycocalyx and the vascular remodeling induced by hemodynamic environment alteration.[20] Although the role of the glycocalyx in mechanotransduction has been extensively studied at the single cellular level, little care has been taken to its potential mechanotransduction role in vascular remodeling at the tissue level.

In an attempting to explain how hemodynamic alteration affects vascular remodeling and elucidate whether the glycocalyx could be a potential mechanosensor, we designed a flow circuit system to apply altered hemodynamic conditions to cultured rat abdominal aorta. Hyaluronidase (HAase) was applied to degrade cells glycocalyx selectively. Vascular remodeling in molecular, cellular, and structural levels were assessed and compared among the following 6 groups of vessels: (1) untreated with no flow and no pressure (control [C]), (2) HAase treatment with no flow and no pressure (HAase+control [HA+C]), (3) untreated with flow and normal pressure (shear+normal pressure [Sh+NP]), (4) HAase treatment with flow and normal pressure (HAase+shear+normal pressure [HA+Sh+NP]), (5) untreated with flow and high pressure (shear+high pressure [Sh+HP]), (6) HAase treatment with flow and high pressure (HAase+shear+high pressure [HA+Sh+HP]).

Materials and Methods

The authors declare that all supporting data are available within the article (online-only Data Supplement).

Vessel Culture

The experiment followed a protocol approved by the institutional committee on animal use in Beihang University, and all animal care was complied with the Principles of Laboratory Animal Care and the Guide for the Care and Use of Laboratory Animals (NIH Publication No. 86-23, Revised 1985). Male Sprague–Dawley rats (specific pathogen free) weighing between 250 and 350 g were anesthetized by intraperitoneal injection of pentobarbital sodium (50 mg/kg). Rat abdominal aortas isolated (online-only Data Supplement) were cultured for 4 days in Dulbecco Modified Eagle Medium supplemented with 10% (volume/volume) fetal bovine serum and 1% penicillin-streptomycin in an organ bath that could be connected to a home-made flow circuit system.

Figure S1 in the online-only Data Supplement is the schematic drawing of the flow circuit system used in the present study. Briefly, the organ bath was mainly made by polypropylene, which had 4 stainless steel stents to secure the vessel. Fluid flow was provided by a peristaltic pump (Longer pump, Hebei, China) and 2 reservoirs situated one above another. Upper reservoir plus the flow stabilizer provides a steady flow to the organ bath. To avoid bacterial contamination, syringe filter was used in this system. Shear stress was determined by the following equation: $\tau=4\ \mu Q/\pi R^3$, where τ is shear stress (dyn/cm^2), μ is the viscosity of culture medium (0.0084 poise), Q is the flow rate across the vascular lumen (mL/s), and R is the luminal radius of vessel (cm). All experimental groups were conducted at 20 dyn/cm^2. This level of shear stress is in the physiological range found in major arteries of rats. Pressure was applied by adjusting the height between organ bath and the upper reservoir. The different experimental groups were conducted at 85 mm Hg (normal pressure) and 135 mm Hg (high pressure). The control group was cultured with or without hyaluronidase treatment in the static condition and was placed side by side with the experimental group at a same organ bath. During the cultured period, the organ bath and reservoir were kept in 95% air and 5% CO_2, 37°C incubator. At the end of the culture, each vessel was cut into 2 parts. One part was immediately placed in RNase-free microfuge tubes and stored at ultra–low-temperature freezer (−80°C) for the following real-time PCR experiments. The other part was stretched to the in situ length and continually perfused with 4% paraformaldehyde solution for 5 minutes at room temperature. After perfusion, the segment was fixed by the same solution overnight and then embedded in Tissue-Tek optimum cutting temperature (OCT; Sakura Finetek USA, Torrance, CA) medium. The embedded samples were frozen quickly and stored at −80°C.

Hyaluronidase Treatment

HAase from bovine testes (Sigma-Aldrich; Type IV-S) was applied to specifically degrade the vascular glycocalyx, which mainly hydrolyzes the HA of glycocalyx but also affects the chondroitin sulfate simultaneously. The enzyme was dissolved in 20 mmol/L sodium phosphate buffer, pH 7.0, containing 77 mmol/L NaCl, 0.1 mg/mL BSA, and stored at −20°C. It was freshly diluted in PBS plus 1% BSA and used at a final concentration of 14 μg/mL.[21] The lumen of the vessel was incubated with this enzyme for 1 hour in organ bath inside a 95% air and 5% CO_2, 37°C incubator. Afterward, the enzyme solution was replaced by culture medium supplemented with 10 μg/mL HAase to inhibit the recovery of the digested glycocalyx.[22,23]

Statistical Analysis

Data are presented as mean±SEM. Statistical analysis was performed by repeated-measures analysis of Student *t* test with a 2-tailed distribution. Each experiment was repeated 3 to 6 times, and results were considered statistically significant with $P<0.05$.

Results

Enzymatic Removal of HA

By using immunofluorescence, the effectiveness of HAase-induced HA cleavage was verified. The fluorescein isothiocyanate–conjugated wheat germ agglutinin specifically labeled the components of glycocalyx on vessel cross sections from intima to adventitia except for the elastic fiber (Figure 1A, 1C, and 1D) and the fluorescein isothiocyanate alone stained nonspecific area of the vessel (Figure 1B). Arrowheads in Figure 1A denote the endothelial glycocalyx above, below, and away from the nucleus.

Figure 1E and 1F shows the fluorescence intensity of the glycocalyx on SMC and EC surface normalized to the control group, respectively. After enzymatic treatment, the glycocalyx distributed on the media and intima was significantly decreased to 59.7±0.7% and 51.0±1.6%, respectively, compared with their control group ($P<0.05$). It should be noted that the medial and endothelial fluorescence intensity of glycocalyx on the vessels cultured for 4 days in culture medium

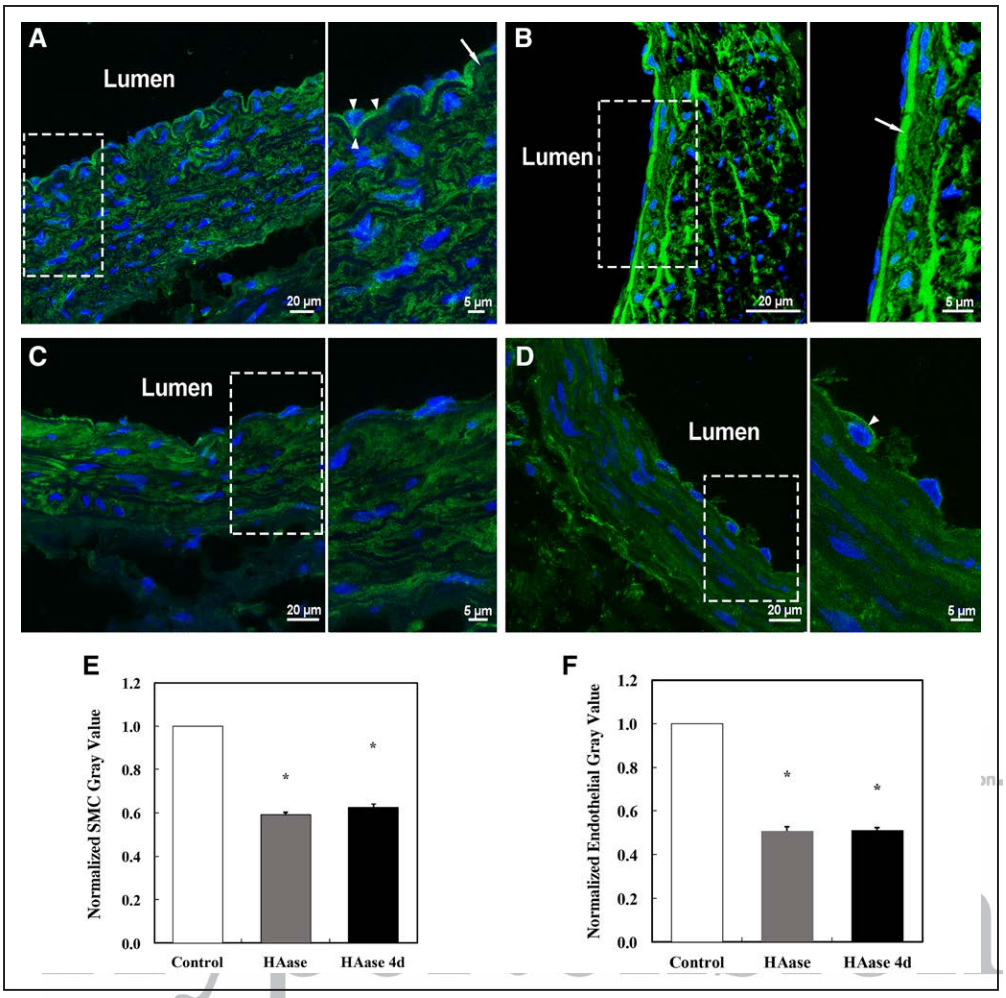

Figure 1. Representative photographs and gray value analysis (**E–F**) of fluorescein isothiocyanate (FITC)–conjugated wheat germ agglutinin staining for nontreatment (**A**), hyaluronidase (HAase) treated (**C**), and 4 d after HAase-treated (**D**) vessels. Negative control was labeled by FITC (**B**). The zoomed images show the boxed area on the left. Arrowheads denote the endothelial glycocalyx above, below, and away from the nucleus, and arrows indicate the internal elastic lamina (IEL). *P<0.05 vs control. HAase 4d indicates HAase treatment group after 4-day culture.

supplemented with 10 μg/mL HAase were 63.1±1.2% and 51.0±1.1%, respectively, which showed no significant differences when compared with the 0-day freshly digested group (HAase).

Glycocalyx Mediates Vessel Morphological Remodeling Induced by Hemodynamic Environmental Alteration

Representative photographs of the hematoxylin and eosin–stained arteries cultured in normal-pressure and high-pressure conditions are shown in Figures 2 and 3, respectively.

The histomorphometric analysis in Figure 3 shows that the exposure of the vessels to shear stress of 20 dyn/cm^2 and pressure of 135 mm Hg for 4 days increased the luminal diameter (D) by 8.5% (shear versus control, P<0.05) and thinned the intima thickness (T_I), the media thickness (T_M), and the whole-vessel wall thickness (T_W, adventitia not included) by 10.3% (shear versus control, P<0.05), 6.7% (shear versus control, P<0.01), and 5.2% (shear versus control, P<0.01), respectively. However, the intimal-media ratio (IMR), the cross-sectional area of the intima (CSA_I), and media (CSA_M) showed no significant between control and shear groups. For the normal-pressure group (Figure 2), shear stress and pressure exposure decreased the D, T_I, T_M, T_W, CSA_I, and CSA_M significantly but insignificantly affect the IMR. Notably, these changes induced by shear stress and pressure were no longer observed after the pretreatment of HAase in both high-pressure group (HAase versus HAase+shear, P>0.24) and normal-pressure group (HAase versus HAase+shear, P>0.09).

Figure 4 shows the fold values of shear/control and HAase+shear/HAase in high- and normal-pressure groups. All experimental groups were normalized with their controls, respectively, to eliminate the differences of experiment time or rat batch. The fold changes of D, T_I, T_M, T_W CSA_M and CSA_I between shear group and control group (shear/control) in high-pressure condition show a significant upregulation relative to the normal-pressure condition, indicating that the high pressure induced the increase of these parameters. However, after the treatment of HAase, the values (HAase+shear/HAase) of all parameters were close to 1 and showed no significant differences between normal- and high-pressure groups. These observations suggested that the

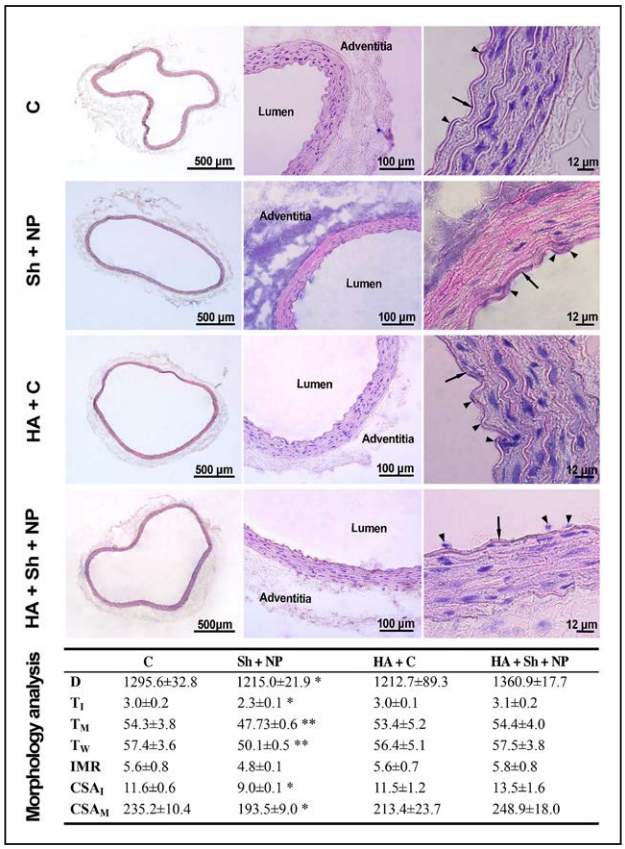

Morphology analysis

	C	Sh + NP	HA + C	HA + Sh + NP
D	1295.6±32.8	1215.0±21.9 *	1212.7±89.3	1360.9±17.7
T_I	3.0±0.2	2.3±0.1 *	3.0±0.1	3.1±0.2
T_M	54.3±3.8	47.73±0.6 **	53.4±5.2	54.4±4.0
T_W	57.4±3.6	50.1±0.5 **	56.4±5.1	57.5±3.8
IMR	5.6±0.8	4.8±0.1	5.6±0.7	5.8±0.8
CSA_I	11.6±0.6	9.0±0.1 *	11.5±1.2	13.5±1.6
CSA_M	235.2±10.4	193.5±9.0 *	213.4±23.7	248.9±18.0

Figure 2. Representative photographs and histomorphometric analysis of vessels stained by hematoxylin and eosin under the normal-pressure condition. Arrowhead denotes the endothelial cells. Arrows show the internal elastic lamina. Data are presented as mean±SEM. $^{**}P<0.01$ vs control (C); $^{*}P<0.05$ vs control. CSA_I indicates the cross-sectional area of the intima ($\mu m^2 \times 10^3$); CSA_M, the cross-sectional area of the media ($\mu m^2 \times 10^3$); D, Luminal diameter (μm); HA, HAase; NP, normal pressure; Sh, shear; T_I, intimal thickness (μm); T_M, medial thickness (μm); T_W, wall thickness (adventitia not included, μm); and IMR: the ratio of intima to media ($\times 10^{-2}$).

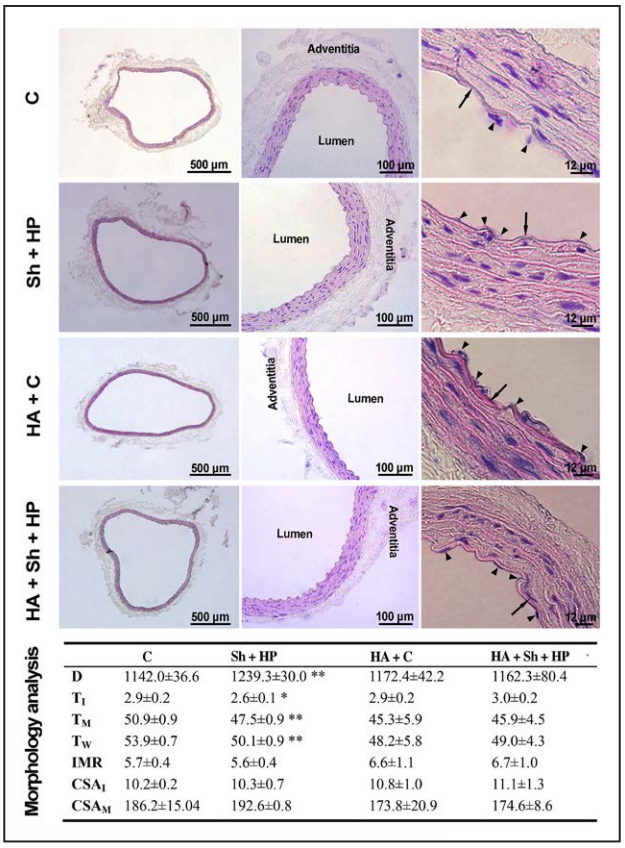

Morphology analysis

	C	Sh + HP	HA + C	HA + Sh + HP
D	1142.0±36.6	1239.3±30.0 **	1172.4±42.2	1162.3±80.4
T_I	2.9±0.2	2.6±0.1 *	2.9±0.2	3.0±0.2
T_M	50.9±0.9	47.5±0.9 **	45.3±5.9	45.9±4.5
T_W	53.9±0.7	50.1±0.9 **	48.2±5.8	49.0±4.3
IMR	5.7±0.4	5.6±0.4	6.6±1.1	6.7±1.0
CSA_I	10.2±0.2	10.3±0.7	10.8±1.0	11.1±1.3
CSA_M	186.2±15.04	192.6±0.8	173.8±20.9	174.6±8.6

Figure 3. Representative photographs and histomorphometric analysis of vessels stained by hematoxylin and eosin under the high-pressure (HP) condition. Arrowhead denotes the endothelial cells. Arrows show the internal elastic lamina. Data are presented as mean±SEM. $^{**}P<0.01$ vs control (C); $^{*}P<0.05$ vs C. CSA_I indicates the cross-sectional area of the intima ($\mu m^2 \times 10^3$); CSA_M, the cross-sectional area of the media ($\mu m^2 \times 10^3$); D, Luminal diameter (μm); HA, HAase; NP, normal pressure; Sh, shear; T_I, intimal thickness (μm); T_M, medial thickness (μm); T_W, wall thickness (adventitia not included, μm); and IMR: the ratio of intima to media ($\times 10^{-2}$).

vessel morphological remodeling induced by hemodynamic environmental alteration could be inhibited when the glycocalyx was degraded.

Glycocalyx Mediates NOS mRNA Expression Induced by Hemodynamic Environmental Alteration

As shown in Figure 5, the mRNA levels of NOSII (inducible NOS) in shear-exposed vessels under normal- and high-pressure conditions showed a respective 2.58±0.98-fold and 2.37±0.73-fold increase relative to the control group. However, after pretreated the vessels with HAase, the mRNA level of NOSII became upregulated significantly in high-pressure condition ($P<0.05$) and showed no significant differences in normal-pressure group ($P>0.51$) with respect to their no enzymatic treated groups. On the other hand, 4-day exposure to the 20 dyn/cm^2 shear stress upregulated NOSIII (endothelial NOS) mRNA levels in both normal- and high-pressure condition. More interestingly, after HAase treatment, the NOSIII expression levels induced by shear stress were significantly downregulated in both the normal-pressure (shear: 5.84±0.88-fold versus HAase+shear: 2.15±0.7-fold, $P<0.05$) and the high-pressure (shear: 4.73±0.55-fold versus HAase+shear: 0.34±0.08-fold, $P<0.01$) groups relative to the respective untreated groups.

Glycocalyx Mediates SMC Contractile Marker Gene mRNA Levels Regulated by Hemodynamic Environmental Alteration

Figure 5 shows the mRNA level of SMC contractile marker genes exposed to 4-day shear stress in normal-pressure, high-pressure, normal-pressure with HAase treatment and high-pressure with HAase treatment. We probed α-SMA (α-smooth muscle actin), SM22 (smooth muscle 22), SMTN (smoothelin), calponion, and GAPDH was used as the internal loading control. The statistical results showed that shear stress exposure upregulated the mRNA levels of α-SMA, SM22, SMTN, and calponion in both normal- and high-pressure conditions relative to the static control group, whereas only SM22 showed significant differences between the normal- and high-pressure group (normal versus high, $P<0.01$). However, the pretreatment of HAase significantly inhibited

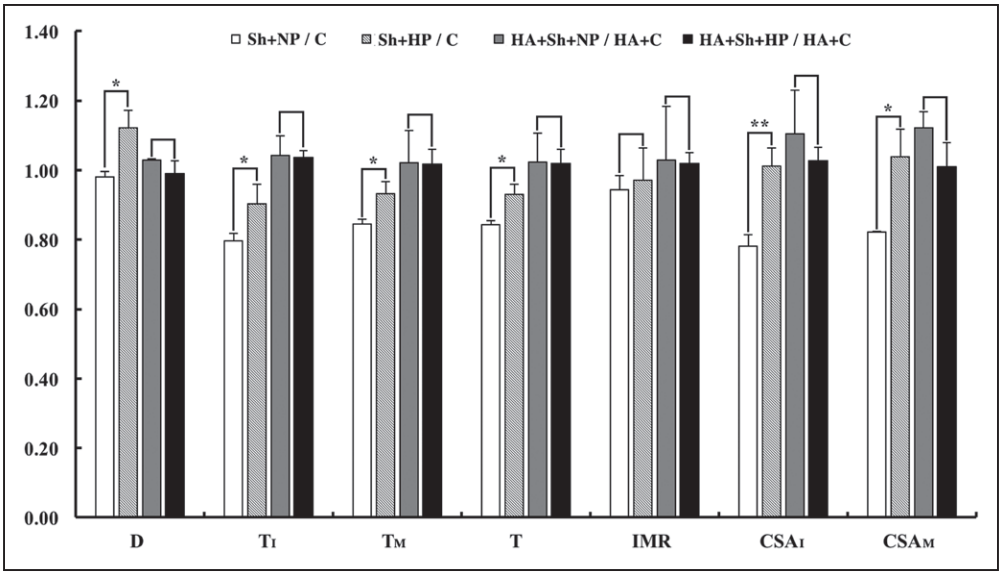

Figure 4. Normalized geometric parameters of vessels exposed to normal-pressure (NP) or high-pressure (HP) conditions. All data were normalized to their controls, respectively. ***P*<0.01 vs parameters in NP; **P*<0.05 vs parameters in NP. CSA_I indicates the cross-sectional area of the intima; CSA_M, the cross-sectional area of the media; D, Luminal diameter; HA, HAase; Sh, shear; T_I, intimal thickness; T_M, medial thickness; T_W, wall thickness (adventitia not included); and IMR: the ratio of intima to media.

the hemodynamic effect for the mRNA levels of α-SMA, SM22, SMTN, and calponion under both normal- and high-pressure conditions. All together, these results suggest that glycocalyx may play a pivotal role in the sensing of hemodynamic environment changes to regulate the expression of SMC contractile marker genes.

Glycocalyx Mediates Apoptosis of SMC Induced by Hemodynamic Environmental Alteration

Figure 6A through 6D illustrates representative immunofluorescence images of TUNEL staining. The nuclei of all vascular cells were stained with DAPI (4',6-diamidino-2-phenylindole), and the apoptotic cells were specifically stained with enzyme solution in situ cell detection kit from Roche (Figure 6A and 6B), whereas in the negative control group, only the nonspecific portion was stained when it incubated by the label solution alone (Figure 6C and D). We counted the number of total (Figure 6E) and apoptotic SMCs of vascular cross sections and calculated the apoptotic rate (Figure 6F). The result showed that both the SMC number and TUNEL-positive cells increased significantly after exposing the vessels to shear and high-pressure conditions (for SMC number, normal: 589.6±37.3 versus high: 732.9±23.4, $P<0.05$; for apoptotic rate, normal: 9.9% ± 2.2% versus high: 20.6% ± 3.7%, $P<0.05$).

However, this enhancement was no longer observed after HAase treatment (for SMC number, normal: 523.4±27.1 versus high: 493.9±44.5, $P>0.67$; for apoptotic rate, normal: 15.1% ± 3.6% versus high: 11.8% ± 2.0%, $P>0.48$). More interestingly, the SMC apoptotic rate showed no significant differences between the control and shear groups in normal-pressure condition (shear versus control, $P>0.70$).

Discussion

Figure 1 shows the fluorescein isothiocyanate-conjugated wheat germ agglutinin staining of the glycocalyx from the intima to adventitia of vessel slices. This kind of staining is consistent with our earlier confocal microscopic observation that fluorescein isothiocyanate–conjugated wheat germ agglutinin specifically labeled the component of the glycocalyx (heparan sulfate, HA, chondroitin sulfate, and sialic acid) from the endothelial and SMCs membrane, extracellular matrix, and cytoplasm.[24] The above, below, and cytoplasmic distribution of endothelial glycocalyx has also been observed by the previous study.[20]

The effectiveness and specificity of HAase for the removal of glycocalyx has been studied extensively during the past 2 decades. van den Berg et al[25] perfused rat heart with 25 IU/mL of hyaluronidase (bovine testis, fraction IV-S; Sigma) for 1 hour at 8 mL/min and clarified that enzyme treatment degraded the hairy-like structures of the glycocalyx into a condensed stained layer but no significant effect on endothelial thickness. More recently, Zeng et al[26] reported that 1.5 U/mL hyaluronidase (from *Streptomyces hyalurolyticus*) treatment of cultured bovine aortic endothelial cells for 2 hours induced a 61.7% reduction in hyaluronic acid. In the present study, the lumen of the vessel was incubated with 14 μg/mL HAase for 1 hour and observed an approximate 49% reduction in the endothelial fluorescence intensity, which seems inconsistent with the results obtained by Zeng et al.[27] The difference of biomarker (Zeng et al:[27] biotinylated hyaluronic acid binding protein versus present study: wheat germ agglutinin) is likely to account for this inconsistence. In addition, Zeng et al[27] reported that S1P (sphingosine 1-phosphate), a sphingolipid in plasma, could induce the recovery of syndecan-1 with attached heparan sulfate and chondroitin sulfate.[27] It may explain the phenomenon that the vessels treated by HAase for 1 hour was detected a portion of glycocalyx regrew after a 4-day culture in medium containing fetal bovine serum (Figure 1D).

The histomophometric and molecular analysis of vessels in the present study suggested a remodeling induced by high pressure, which is consistent with the classic hypertensive

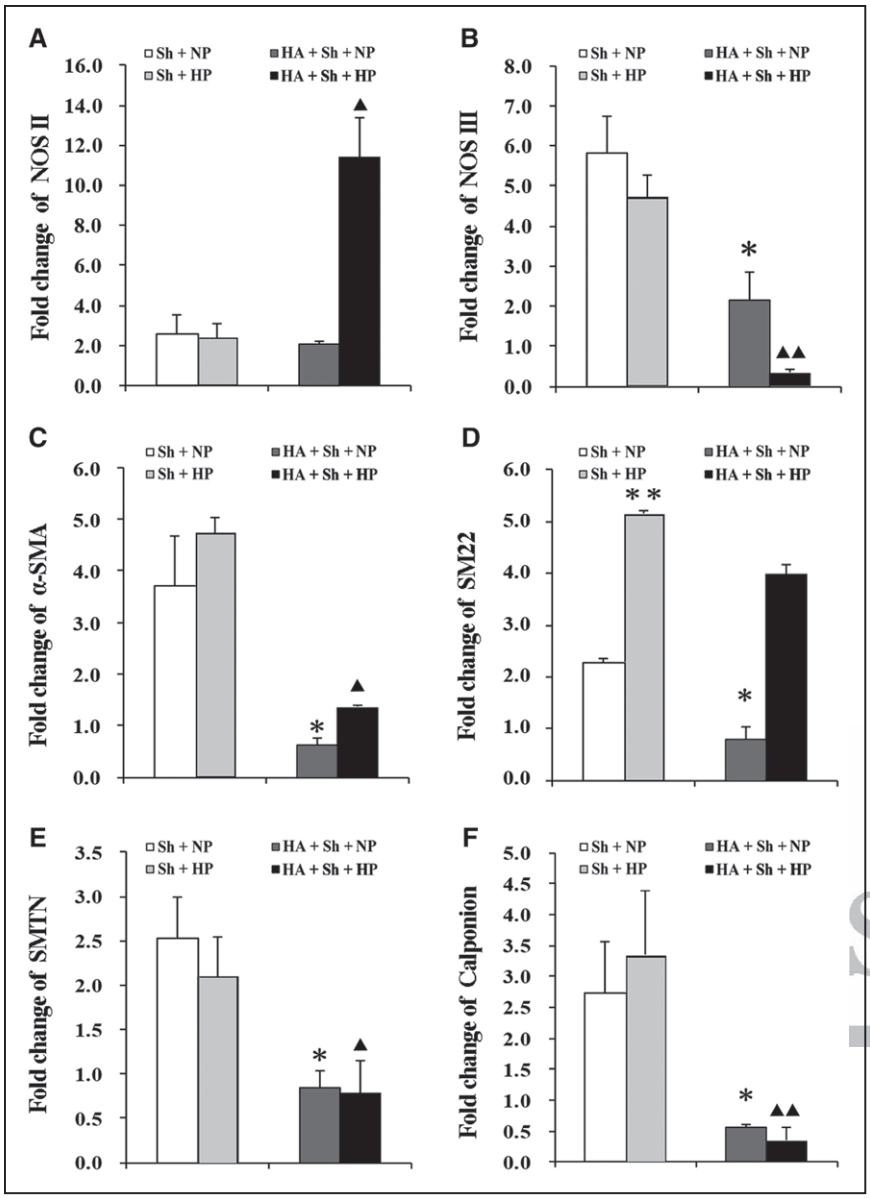

Figure 5. Fold change of NOS (nitric oxide synthase) II, NOSIII, and SMCs (smooth muscle cells) contractile marker gene mRNA levels under normal-pressure (NP) and high-pressure (HP) conditions. The expression was measured by real-time PCR and quantified by a $2^{-\Delta\Delta Ct}$ method. $^{**}P<0.01$ vs shear (Sh) in NP; $^{*}P<0.05$ vs Sh in NP; $^{▲▲}P<0.01$ vs Sh in high pressure (HP); $^{▲}P<0.05$ vs Sh in HP. SM22 indicates SM22 smooth muscle 22.

aortic phenotype characterized by a thicker and more rigid vascular wall as well as increased aortic diameter.[28] Boutouyrie et al[29] noninvasively determined the intima-media thickness and internal diameter of the carotid and radial arteries in healthy subjects and never-treated hypertensive patients with high-definition echo-tracking devices. By establishing multivariate regression models, they discovered that carotid artery enlargement and wall thickening were correlated with pressure independent of age and sex, which are consistent with the results from the present study (Figure 4). These findings accorded with the Glagov's phenomenon[30] and was also observed by Chironi et al.[31] In their experiments, the vessels exhibit hypertrophic outward (determined by increases in both lumen and vessel size) remodeling in hypertension. In addition, Zarins et al[32] observed that cardiovascular diseases within the arterial tree lead to local flow instabilities and separations, which can be detected and visualized as changes as IMR. Moreover, such cardiovascular lesions have been found to be positive correlation with IMR.[33] In the present study, the IMR showed no significant differences between normal pressure and high pressure. This phenomenon suggests that the 4-day culture in high-pressure condition would not change the resistance of their arterial walls against cardiovascular risk factors.[20]

The increased thickness of the vascular wall is likely associated with the proliferation, motility, and secretion capacity of vascular smooth muscle cells. Korshunov and Berk[15] observed that carotid intima-media thickening accompanied by a rapid proliferation of vascular smooth muscle cells, which is consist with our results shown in the Figure 6E where the cell number of vessel significantly increased ($P<0.05$) after loading the high pressure. Furthermore, phenotypic modulation is one of the key events for SMC to be engaged in vascular remodeling. Stegemann et al[34] reported that the phenotype of SMCs is a continuum, and its marker expression decided either a contractile or a synthetic state. In an intact artery, the SMCs are continuously exposed to shear stress due to interstitial flow which

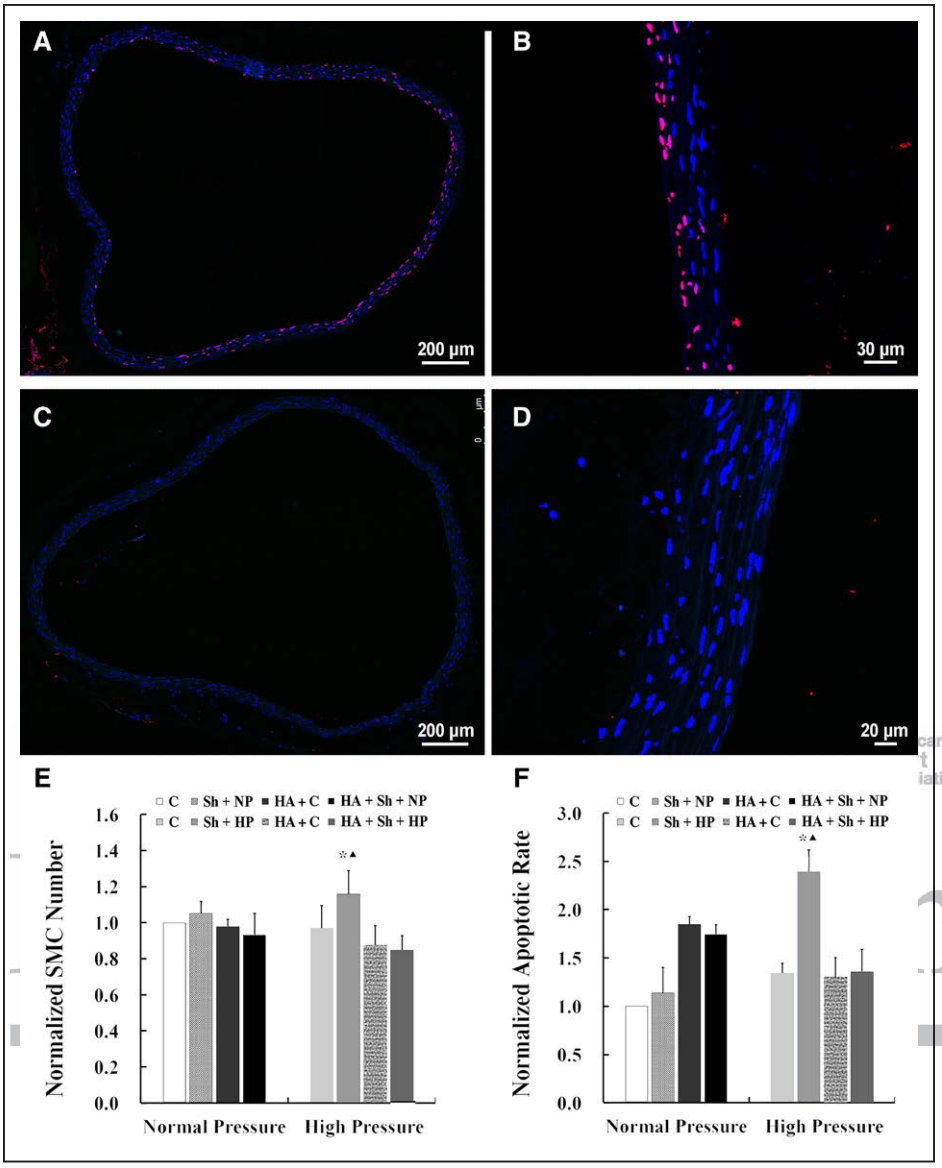

Figure 6. Representative photographs of vessels stained with TUNEL method. **A** and **B**, The apoptotic cells from shear + high-pressure (Sh+HP) group were specifically stained. **C** and **D**, Images of negative group (staining control [C]). **E**, Normalized number of SMCs (smooth muscle cells) of vascular cross sections. **F**, Normalized apoptotic rate of SMCs. The C and hyaluronic acid (HA)+C in normal-pressure (NP) and HP conditions are both the untreated and HAase-treated groups with no flow and no pressure but produced in different times to eliminate the differences of rat batch. **P*<0.05 vs C in HP; ▲*P*<0.05 vs Sh in NP.

is positively related to the transmural pressure. Shi et al[5] showed that enhanced interstitial flow induced the expression of SMC marker gene *SM22*, which is consistent with the results from Figure 5. However, our observation that the α-SMA, SMTN and Calponion showed no significant differences between the normal and high pressure groups was contradictory to the studies from Shi et al.[5] It may be attributed to the differences in the loading method and shear stress values of interstitial flow. In addition, recent reports indicated that NOS isoforms play a significant role in vascular remodeling where nitric oxide (NO) derived from NOSIII (endothelial NOS) inhibits intima formation and NO derived from NOSII (inducible NOS) suppresses the development of remodeling.[35] Consistent with this, we observed a remarkable increase in the mRNA levels of NOSII and NOSIII induced by hemodynamic environment changes. More interestingly, in our experiment, a significant enhancement of SMC apoptosis rate after exposing the vessels to shear stress and high pressure condition was observed. This phenomenon may be explained by a compensation mechanism that some forms of hypertension may be compensated or modified by countervailing mechanisms, particularly apoptosis.[36] Devlin et al[37] and Rizzoni et al[38] have reported that vascular smooth muscle cells are more prone to apoptosis in spontaneously hypertensive rats (SHR), which seems consistent with the present study.

As collective evidence in our present study shown, glycocalyx may play a very important role in the vascular remodeling induced by altered hemodynamic environment. Mechanisms underlying remain to be elucidated and recent studies have

provided insight into some of the factors and pathways that may be involved. According to Shi et al,[5] glycocalyx-mediated ERK1/2 (extracellular regulated protein kinases 1/2) activation is an important pathway in modulating SMC marker gene expression, proliferation, and apoptosis when SMCs are exposed to interstitial flow, which substantiated the mechanotransduction role of the glycocalyx in interstitial flow-induced cellular processes. It may explain the results in our experiment that the effects of hemodynamic environment changes on SMC marker genes and apoptotic rate disappeared after compromising the integrity of glycocalyx. Moreover, NO production and bioavailability are bound up with regulating the vasoconstriction and vasodilation, and their alteration promote the vascular remodeling process.[36] Our previous studies have demonstrated that glycocalyx participates in mechanosensing that mediates NO production and NO synthase activation in response to shear stress.[18] More recently, Mochizuki et al[39] perfused the isolated canine femoral arteries with a Krebs–Henseleit solution at a wide range of perfusion rates with and without pretreatment with HAase to degrade HA within the glycocalyx layer. By quantifying the differential product of nitrite concentration, they found that HAase treatment significantly decreased flow-induced NO production. Although 2 different samples were used, rat abdominal aorta versus canine femoral arteries, we and Mochizuki et al[39] all observed the evidence that the glycocalyx is a possible biomechanical sensor that triggers NO production by transmitting hemodynamic environment changes to the vessel.

It should be noted that all results obtained after enzymatic treatment in the present study were resulted from the digestion of the glycocalyx on both intima and media. Therefore, it should be viewed as the glycocalyx-mediated effect at a tissue level and was impossible to distinguish the EC effect or SMC effect alone. Researches on the interaction between SMC and EC are a classical topic in cardiovascular pathophysiology. Antonelli et al[40] and Fillinger et al[41] used in vitro coculture system to mimic the cells of the vessel wall and examined the interactions between SMC and EC. More recently, Korff et al[42] investigated blood vessel maturation processes in a novel 3D spheroidal coculture system of EC and SMC. In the present study, we did not carry out further studies on the interaction between SMC and EC. However, the flow circuit system in this article is an ideal device for the topic. We are considering using this technique in our future study to dig more interesting topic and conduct studies deeply.

Perspectives

In the present study, the vascular remodeling induced by hemodynamic environmental alteration by a home-made vessel culture system was investigated. The results indicated that the vessel cultured under high-pressure condition showed a remodeling that is consistent with the classic hypertensive aortic phenotypes. However, those phenomena induced by hemodynamic environmental changes are totally abolished after compromising the integrity of glycocalyx by the treatment of vessels with HAase. Although the mechanisms responsible for this remain unclear, our results suggested that glycocalyx may play a pivotal role in mechanotransduction of this kind of hemodynamic environmental alteration in the process of vascular remodeling. This provides a new insight into the therapeutic strategies that will intervene with the processes resulting in the major vascular disorders such as arterial hypertension, atherosclerosis, and other cardiovascular diseases.

Acknowledgments

We acknowledge Zhenze Wang, Xiao Liu, Ping Zhao, and Qinghua Hu for providing help on the flow circuit system.

Sources of Funding

This work was supported by Grants-in-Aid from the National Natural Science Foundation of China (Nos. 31500763, 11772036, 11572028, 11472031, 11421202), National Key Research and Development Program in China (No. 2017YFB0702501), and the Fundamental Research Funds for the Central Universities.

Disclosures

None.

References

1. Gibbons GH, Dzau VJ. The emerging concept of vascular remodeling. *N Engl J Med*. 1994;330:1431–1438. doi: 10.1056/NEJM199405193302008.
2. Short D. The vascular fault in chronic hypertension with particular reference to the role of medial hypertrophy. *Lancet*. 1966;1:1302–1304.
3. Baumbach GL, Heistad DD. Remodeling of cerebral arterioles in chronic hypertension. *Hypertension*. 1989;13(6 pt 2):968–972.
4. Dickhout JG, Lee RM. Structural and functional analysis of small arteries from young spontaneously hypertensive rats. *Hypertension*. 1997;29:781–789.
5. Shi ZD, Abraham G, Tarbell JM. Shear stress modulation of smooth muscle cell marker genes in 2-D and 3-D depends on mechanotransduction by heparan sulfate proteoglycans and ERK1/2. *PLoS One*. 2010;5:e12196. doi: 10.1371/journal.pone.0012196.
6. Taddei S, Virdis A, Mattei P, Ghiadoni L, Gennari A, Fasolo CB, Sudano I, Salvetti A. Aging and endothelial function in normotensive subjects and patients with essential hypertension. *Circulation*. 1995;91:1981–1987.
7. Wang Y, Zhang M, Liu Y, Liu Y, Chen M. The effect of nebivolol on asymmetric dimethylarginine system in spontaneously hypertension rats. *Vascul Pharmacol*. 2011;54:36–43. doi: 10.1016/j.vph.2010.12.001.
8. Osol G, Moore LG. Maternal uterine vascular remodeling during pregnancy. *Microcirculation*. 2014;21:38–47. doi: 10.1111/micc.12080.
9. Han DK, Haudenschild CC, Hong MK, Tinkle BT, Leon MB, Liau G. Evidence for apoptosis in human atherogenesis and in a rat vascular injury model. *Am J Pathol*. 1995;147:267–277.
10. Prior BM, Lloyd PG, Yang HT, Terjung RL. Exercise-induced vascular remodeling. *Exerc Sport Sci Rev*. 2003;31:26–33.
11. Schiffrin EL. Vascular remodeling in hypertension: mechanisms and treatment. *Hypertension*. 2012;59:367–374. doi: 10.1161/HYPERTENSIONAHA.111.187021.
12. Dzau VJ, Gibbons GH, Morishita R, Pratt RE. New perspectives in hypertension research. Potentials of vascular biology. *Hypertension*. 1994;23(6 pt 2):1132–1140.
13. Montezano AC, Tsiropoulou S, Dulak-Lis M, Harvey A, Camargo Lde L, Touyz RM. Redox signaling, Nox5 and vascular remodeling in hypertension. *Curr Opin Nephrol Hypertens*. 2015;24:425–433. doi: 10.1097/MNH.0000000000000153.
14. Grassi G, Ram VS. Evidence for a critical role of the sympathetic nervous system in hypertension. *J Am Soc Hypertens*. 2016;10:457–466. doi: 10.1016/j.jash.2016.02.015.
15. Korshunov VA, Berk BC. Flow-induced vascular remodeling in the mouse: a model for carotid intima-media thickening. *Arterioscler Thromb Vasc Biol*. 2003;23:2185–2191. doi: 10.1161/01.ATV.0000103120.06092.14.
16. Pahakis MY, Kosky JR, Dull RO, Tarbell JM. The role of endothelial glycocalyx components in mechanotransduction of fluid shear stress. *Biochem Biophys Res Commun*. 2007;355:228–233. doi: 10.1016/j.bbrc.2007.01.137.
17. Weinbaum S, Zhang X, Han Y, Vink H, Cowin SC. Mechanotransduction and flow across the endothelial glycocalyx. *Proc Natl Acad Sci USA*. 2003;100:7988–7995. doi: 10.1073/pnas.1332808100.
18. Kang H, Fan Y, Deng X. Vascular smooth muscle cell glycocalyx modulates shear-induced proliferation, migration, and NO production

responses. *Am J Physiol Heart Circ Physiol*. 2011;300:H76–H83. doi: 10.1152/ajpheart.00905.2010.
19. Shi ZD, Wang H, Tarbell JM. Heparan sulfate proteoglycans mediate interstitial flow mechanotransduction regulating MMP-13 expression and cell motility via FAK-ERK in 3D collagen. *PLoS One*. 2011;6:e15956. doi: 10.1371/journal.pone.0015956.
20. Kang H, Sun L, Huang Y, Wang Z, Zhao P, Fan Y, Deng X. Regional specific adaptation of the endothelial glycocalyx dimension in tail-suspended rats. *Pflugers Arch*. 2015;467:1291–1301. doi: 10.1007/s00424-014-1568-1.
21. Kumagai R, Lu X, Kassab GS. Role of glycocalyx in flow-induced production of nitric oxide and reactive oxygen species. *Free Radic Biol Med*. 2009;47:600–607. doi: 10.1016/j.freeradbiomed.2009.05.034.
22. Barker AL, Konopatskaya O, Neal CR, Macpherson JV, Whatmore JL, Winlove CP, Unwin PR, Shore AC. Observation and characterisation of the glycocalyx of viable human endothelial cells using confocal laser scanning microscopy. *Phys Chem Chem Phys*. 2004;6:1006–1011.
23. Meuwese MC, Broekhuizen LN, Kuikhoven M, Heeneman S, Lutgens E, Gijbels MJ, Nieuwdorp M, Peutz CJ, Stroes ES, Vink H, van den Berg BM. Endothelial surface layer degradation by chronic hyaluronidase infusion induces proteinuria in apolipoprotein E-deficient mice. *PLoS One*. 2010;5:e14262. doi: 10.1371/journal.pone.0014262.
24. Kang H, Fan Y, Zhao P, Ren C, Wang Z, Deng X. Regional specific modulation of the glycocalyx and smooth muscle cell contractile apparatus in conduit arteries of tail-suspended rats. *J Appl Physiol (1985)*. 2016;120:537–545. doi: 10.1152/japplphysiol.00245.2015.
25. van den Berg BM, Vink H, Spaan JA. The endothelial glycocalyx protects against myocardial edema. *Circ Res*. 2003;92:592–594. doi: 10.1161/01.RES.0000065917.53950.75.
26. Zeng Y, Ebong EE, Fu BM, Tarbell JM. The structural stability of the endothelial glycocalyx after enzymatic removal of glycosaminoglycans. *PLoS One*. 2012;7:e43168. doi: 10.1371/journal.pone.0043168.
27. Zeng Y, Liu XH, Tarbell J, Fu B. Sphingosine 1-phosphate induced synthesis of glycocalyx on endothelial cells. *Exp Cell Res*. 2015;339:90–95. doi: 10.1016/j.yexcr.2015.08.013.
28. Wiener J, Loud AV, Giacomelli F, Anversa P. Morphometric analysis of hypertension-induced hypertrophy of rat thoracic aorta. *Am J Pathol*. 1977;88:619–634.
29. Boutouyrie P, Bussy C, Lacolley P, Girerd X, Laloux B, Laurent S. Association between local pulse pressure, mean blood pressure, and large-artery remodeling. *Circulation*. 1999;100:1387–1393.
30. Korshunov VA, Schwartz SM, Berk BC. Vascular remodeling: hemodynamic and biochemical mechanisms underlying Glagov's phenomenon. *Arterioscler Thromb Vasc Biol*. 2007;27:1722–1728. doi: 10.1161/ATVBAHA.106.129254.
31. Chironi G, Gariepy J, Denarie N, Balice M, Megnien JL, Levenson J, Simon A. Influence of hypertension on early carotid artery remodeling. *Arterioscler Thromb Vasc Biol*. 2003;23:1460–1464. doi: 10.1161/01.ATV.0000083342.98342.22.
32. Zarins CK, Giddens DP, Bharadvaj BK, Sottiurai VS, Mabon RF, Glagov S. Carotid bifurcation atherosclerosis. Quantitative correlation of plaque localization with flow velocity profiles and wall shear stress. *Circ Res*. 1983;53:502–514.
33. van den Berg BM, Spaan JA, Rolf TM, Vink H. Atherogenic region and diet diminish glycocalyx dimension and increase intima-to-media ratios at murine carotid artery bifurcation. *Am J Physiol Heart Circ Physiol*. 2006;290:H915–H920. doi: 10.1152/ajpheart.00051.2005.
34. Stegemann JP, Hong H, Nerem RM. Mechanical, biochemical, and extracellular matrix effects on vascular smooth muscle cell phenotype. *J Appl Physiol (1985)*. 2005;98:2321–2327. doi: 10.1152/japplphysiol.01114.2004.
35. Yogo K, Shimokawa H, Funakoshi H, Kandabashi T, Miyata K, Okamoto S, Egashira K, Huang P, Akaike T, Takeshita A. Different vasculoprotective roles of NO synthase isoforms in vascular lesion formation in mice. *Arterioscler Thromb Vasc Biol*. 2000;20:E96–E100.
36. Intengan HD, Schiffrin EL. Vascular remodeling in hypertension: roles of apoptosis, inflammation, and fibrosis. *Hypertension*. 2001;38(3 pt 2):581–587.
37. Devlin AM, Clark JS, Reid JL, Dominiczak AF. DNA synthesis and apoptosis in smooth muscle cells from a model of genetic hypertension. *Hypertension*. 2000;36:110–115.
38. Rizzoni D, Rodella L, Porteri E, Rezzani R, Guelfi D, Piccoli A, Castellano M, Muiesan ML, Bianchi R, Rosei EA. Time course of apoptosis in small resistance arteries of spontaneously hypertensive rats. *J Hypertens*. 2000;18:885–891.
39. Mochizuki S, Vink H, Hiramatsu O, Kajita T, Shigeto F, Spaan JA, Kajiya F. Role of hyaluronic acid glycosaminoglycans in shear-induced endothelium-derived nitric oxide release. *Am J Physiol Heart Circ Physiol*. 2003;285:H722–H726. doi: 10.1152/ajpheart.00691.2002.
40. Antonelli-Orlidge A, Saunders KB, Smith SR, D'Amore PA. An activated form of transforming growth factor beta is produced by cocultures of endothelial cells and pericytes. *Proc Natl Acad Sci USA*. 1989;86:4544–4548.
41. Fillinger MF, O'Connor SE, Wagner RJ, Cronenwett JL. The effect of endothelial cell coculture on smooth muscle cell proliferation. *J Vasc Surg*. 1993;17:1058–1067; discussion 1067.
42. Korff T, Kimmina S, Martiny-Baron G, Augustin HG. Blood vessel maturation in a 3-dimensional spheroidal coculture model: direct contact with smooth muscle cells regulates endothelial cell quiescence and abrogates VEGF responsiveness. *FASEB J*. 2001;15:447–457. doi: 10.1096/fj.00-0139com.

Novelty and Significance

What Is New?

- Many biomechanical and biochemical factors are associated with vascular remodeling especially the hemodynamic disturbances. This article designed a flow circuit system and provided evidence of the important mechanotransduction role of the vascular cells glycocalyx in vascular remodeling induced by hemodynamic environmental alteration (pressure and shear stress).

What Is Relevant?

- Providing a new insight and potential target into the therapeutic strategies that will intervene with the processes resulting in the major vascular disorders such as arterial hypertension, atherosclerosis, and other cardiovascular diseases.

Summary

The vessel cultured in shear and high-pressure condition showed a remodeling in structural, cellular, and molecular levels that are consistent with the classic hypertensive aortic phenotypes. However, those phenomena induced by hemodynamic environmental changes are totally abolished after compromising the integrity of glycocalyx by the treatment of vessels with HAase.

Hypertension
Journal of the American Heart Association

Vascular Cell Glycocalyx-Mediated Vascular Remodeling Induced by Hemodynamic Environmental Alteration

Jiajia Liu, Hongyan Kang, Xuejiao Ma, Anqiang Sun, Huiqin Luan, Xiaoyan Deng and Yubo Fan

Hypertension. published online April 30, 2018;
Hypertension is published by the American Heart Association, 7272 Greenville Avenue, Dallas, TX 75231

Print ISSN: 0194-911X. Online ISSN: 1524-4563

Vascular Cell Glycocalyx Mediated Vascular Remodeling Induced by Hemodynamic Environmental Alteration

Jiajia Liu[a, c], Hongyan Kang[a, c, *], Xuejiao Ma[a, c], Anqiang Sun[a, c], Huiqin Luan[b], Xiaoyan Deng[a, c], Yubo Fan[a, b, c, *]

a Key Laboratory for Biomechanics and Mechanobiology of Ministry of Education, School of Biological Science and Medical Engineering, Beihang University, Beijing, China 100083

b National Research Center for Rehabilitation Technical Aids, Beijing, China 100176

c Beijing Advanced Innovation Centre for Biomedical Engineering, Beihang University, Beijing, China 102402

* Corresponding Author: Dr. Hongyan Kang, School of Biological Science and Medical Engineering, Beihang University, Beijing, China, hongyankang@buaa.edu.cn; Prof. Yubo Fan, National Research Center for Rehabilitation Technical Aids, Beijing, China, Tel: 86-10-82339428; Fax: 86-10-82339428; yubofan@buaa.edu.cn.

Note: Jiajia Liu, School of Biological Science and Medical Engineering, Beihang University, Beijing, China, huicheljj@163.com, is designated as the corresponding author during the manuscript submission and processing, and Dr. Yubo Fan and Hongyan Kang is the corresponding author in the final article

Online Supplement

Materials and Methods

Vessel isolation

Segments of abdominal aorta were excised under sterile conditions from the rats, cannulated with stainless steel tubes (outer diameters 1mm) in both ends, stretched and secured to their in situ length, perfused with culture medium, and transferred to an organ bath immediately.[1] To avoid abnormal leakage of perfusion, the small branches of abdominal aorta were ligated by sterile suture. To avoid dehydration, the required segments of vessel were bathed in stroke-physiological saline (SPSS) during the operation.

Frozen-section

The frozen vessel embedded in OCT was sliced into 6 μm sections by using freezing microtome (Leica Biosystems CM1950, Shanghai, China). Then the sections were mounted on superfrost plus microscope slides (Thermo Scientific, Portsmouth, New Hampshire), exposed to air, dried overnight, and stored at ultra low temperature freezer for the following staining.

Artery glycocalyx immunostaining and quantification

For the glycocalyx staining, the frozen sections were first warmed at room temperature for 10 min, post-fixed in 4 % PFA solution for 10 min, washed twice in PBS (no calcium/magnesium), and treated with antigen retrieval solution (Solarbio, Beijing, China) for 5 min. Following washing in PBS at least three times with 5 min interval, the sliders were treated with 30% H_2O_2 for 20 min, then incubated with fluorescein isothiocyanate-labeled wheat germ agglutinin (WGA-FITC, Sigma Aldrich, St. Louis, MO) at 5 μg/ml for 2h at room temperature. After washing three times in PBS, slides were mounted with Antifade mounting medium with DAPI (HelixGen, Guangzhou, China) for viewing. To verify the specificity of WGA-FITC for the GCX, one negative control was prepared with FITC staining.

All samples were examined using laser scanning confocal microscopy (Leica TCS SP8 MP, Germany) with a 40× oil objective lens. The excitation wavelength of WGA-FITC and DAPI were 448 and 404 nm, respectively, the emission were 510-550 nm and 454 nm, respectively. Images were collected either from the top (near lens) to the bottom or from the bottom to the top (z-direction) for each sample, forming a stack of images along the z-direction. The thickness of each image was 0.15-0.25 μm. For each slice, more than three fields of view were collected, and for each vessel, three to five slices were chosen to compare the gray value of the GCX.

Image J software (National Institute of Health, USA) was used to quantify the gray value of the GCX. The total and endothelial gray value of GCX were measured respectively.

Histology

Histological change was visualized by the method of hematoxylin and eosin (H-E) staining. Briefly, the vessel cross sections were fixed in 4% PFA for 10 min, washed twice in

PBS, and permeabilized with 0.3% Triton X-100 in PBS for 10 min. After which the slides were washed twice with PBS, stained with hematoxylin and eosin for 5 min and 6 min, respectively. After washing three times in PBS, sections were mounted with glycerol-PBS and covered by coverslips, then examined and photographed under an Olympus BX51 light microscope (Olympus America Inc., Melville, New York) with 10×, 20×, and 40× objective lens, respectively.

According to the method described by Wiener[2], the luminal diameter (D), the intimal thickness (T_I) and medial thickness ($T_{M)}$, the ratio of intima to media (IMR), the cross-sectional area of the intima (CSA_I) and media (CSA_M) were measured by Image J software. The parameters D was calculated by using the inner perimeter divided by π. The T_I and T_M were determined by averaging six measurements on each section selected at 0°, 90°, 180°, and 270° along the circumference of each arterial ring. Based on these parameters, T_W (wall thickness, adventitia not included), IMR, CSA_I and CSA_M were calculated by the formulas, $T_W = T_I+T_M$, $IMR = T_I/T_M$, $CSA_I = \pi [(D/2 + T_I)^2 - (D/2)^2]$ and $CSA_M = \pi [(D/2+T_W)^2 - (D/2+T_I)^2]$, respectively.

Real-time PCR

For Real-time PCR experiments, the total RNA of vessel from each sample was isolated with TRNzol reagent according to the manufacturer's instructions. The amount of total RNA from each sample was quantified using a NanoDrop 2000 spectrophotometer (Thermo Scientific, Delaware, USA). Thereafter, 1000 ng total RNA of each sample was reversely transcripted into cDNA using the PrimeScript^{TM} RT reagent Kit (Takara Bio INC., Otsu, Japan). The cDNA was amplified on iQ5 Multicolor Real Time PCR Detection System (Bio-Rad, Hercules, CA) and the reactions were performed in 25 ml reaction mixture volumes containing SYBR Green master mix (Takara Bio INC., Otsu, Japan) and gene-specific primer pairs (Table S1). PCR protocol was as follows: 95°C for 30s at initial denaturation stage, 40 cycles of 95°C for 10s and 60°C for 30s at PCR reaction stage, and followed by dissociation stage. The dissociation curve analysis was used to assess the specificity of product amplification.

Quantification of the relative changes in mRNA levels between different samples was performed using the delta delta threshold cycle (ΔΔCt) method. GAPDH served as an internal control, ΔCt was calculated by subtracting the Ct value of the genes from the Ct value of the GAPDH. ΔΔCt was obtained by subtracting the ΔCt value of the control groups from the ΔCt value of pre-treated groups in the same experiment. Fold change was then calculated as $2^{-\Delta\Delta Ct}$.

TUNEL

Apoptotic SMC of vessel were identified by the terminal deoxynucleotidyl transferase dUTP nick end labeling (TUNEL) technique. The frozen sections were stained using the in situ cell detection kit from Roche (Indianapolis, IN) according to the method described by Cancel et al.[3]. All samples were examined using laser scanning confocal microscopy (Leica TCS SP8 MP, Germany) with 10× objective lens and 40× oil objective lens. The excitation wavelengths of total and apoptotic cells were 404 and 552 nm, respectively, and the emission were 570-620 nm and 454 nm, respectively. SMC apoptotic rates were determined by counting the number

of total and apoptotic SMCs in four to six vessel cross sections of each sample and calculating the average ratio (apoptotic cells number/ total cells number) for each group. After that, the average ratios of all experimental groups were normalized by the data of control group in which the vessels were cultured in a static situation.

References

1. Bolz SS, Pieperhoff S, De Wit C, Pohl U. Intact endothelial and smooth muscle function in small resistance arteries after 48 h in vessel culture. *Am J Physiol Heart Circ Physiol*. 2000;279(3):H1434–9.
2. Wiener J, Loud AV, Giacomelli F, Anversa P. Morphometric analysis of hypertension-induced hypertrophy of rat thoracic aorta. *Am J Pathol*. 1977;88(3):619–634.
3. Cancel LM, Ebong EE, Mensah S, Hirshberg C, Tarbell JM. Endothelial glycocalyx, apoptosis and inflammation in an atherosclerotic mouse model. *Atherosclerosis*. 2016;252:136–146.
4. Slyvka Y, Wang Z, Yee J, Inman SR, Nowak FV. Antioxidant diet, gender and age affect renal expression of nitric oxide synthases in obese diabetic rats. *Nitric Oxide*. 2011;24(1):50–60.
5. Park F, Mattson DL, Roberts LA, Cowley AW, Jr. Evidence for the presence of smooth muscle alpha-actin within pericytes of the renal medulla. *Am J Physiol*. 1997;273:R1742–1748.
6. Tsai RY, McKay RD. Cell contact regulates fate choice by cortical stem cells. J Neurosci. 2000;20:3725–3735.
7. Rensen SS, Niessen PM, Long X, Doevendans PA, Miano JM, van Eys GJ. Contribution of serum response factor and myocardin to transcriptional regulation of smoothelins. *Cardiovasc Res*. 2006;70:136–145.
8. Oishi K, Ogawa Y, Gamoh S, Uchida MK. Contractile responses of smooth muscle cells differentiated from rat neural stem cells. *J Physiol*. 2002;540:139–152.
9. Tao X, Ming-Kun Y, Wei-Bin S, Hai-Long G, Rui K, Lai-Yong T. Role of telomerase reverse transcriptase in glial scar formation after spinal cord injury in rats. *Neurochem Res*. 2013;38(9):1914–20.

Table S1 Primers for PCR Amplification

Gene name	*GenBank Locus*	*Sequence of primers (5'-3')*	*Reference*
NOSII	NC 005109.4	Forward: TGCCCCTGGAAGTTTCTC Reverse: GGTCATCCTGTGTTGTTGG	4
NOSIII	NC 005103.4	Forward: CGGTACTACTCTGTCAGCTCAGC Reverse: CATCCTGGGTTCTGTATGCC	4
α-SMA	NM 031004.2	Forward: GATCACCATCGGGAATGAACGC Reverse: CTTAGAAGCATTTGCGGTGGAC	5
SM22	NM 031549.2	Forward: TGTTCCAGACTGTTGACCTC Reverse: GTGATACCTCAAAGCTGTCC	6
SMTN	NM 001013049	Forward: TCGGAGTGCTGGTGAATAC Reverse: CCCTGTTTCTCTTCCTCTGG	7
Calponion	NM_031747.1	Forward: ACAAAAGGAAACAAAGTCAAT Reverse: GGGCAGCCCATACACCGTCAT	8
GAPDH	NC 005103.4	Forward: GCTCTCTGCTCCTCCCTGTTCT Reverse: CAGGCGTCCGATACGGCCAAA	9

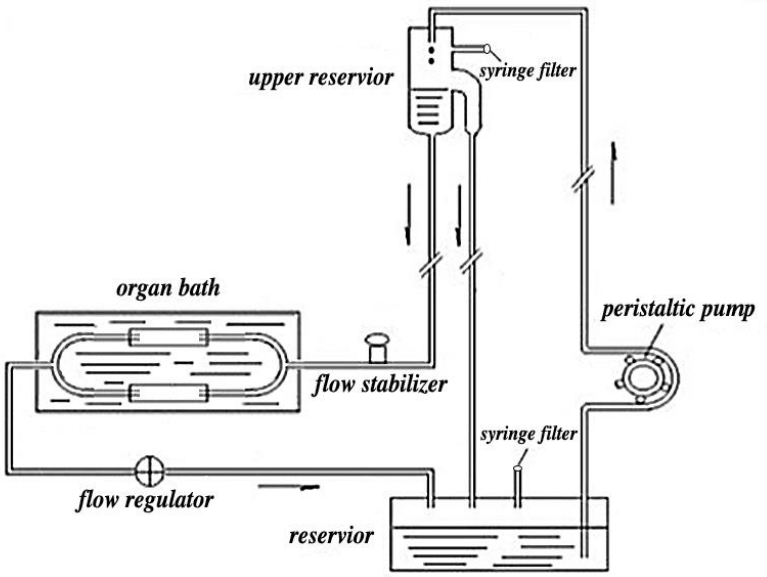

Figure S1 Schematic drawing of the experimental set-up.